Ion Selectivity Filter Regulates Local Anesthetic Inhibition of G-Protein-Gated Inwardly Rectifying K$^+$ Channels

Paul A. Slesinger

The Salk Institute for Biological Studies, Peptide Biology Lab, La Jolla, California 92037 USA

ABSTRACT   The *weaver* mutation (G156S) in G-protein-gated inwardly rectifying K$^+$ (GIRK) channels alters ion selectivity and reveals sensitivity to inhibition by a charged local anesthetic, QX-314, applied extracellularly. In this paper, disrupting the ion selectivity in another GIRK channel, chimera I1G1(M), generates a GIRK channel that is also inhibited by extracellular local anesthetics. I1G1(M) is a chimera of IRK1 (G-protein-insensitive) and GIRK1 and contains the hydrophobic domains (M1–pore-loop–M2) of GIRK1 (G1(M)) with the N- and C-terminal domains of IRK1 (I1). The local anesthetic binding site in I1G1(M) is indistinguishable from that in GIRK2^{wv} channels. Whereas chimera I1G1(M) loses K$^+$ selectivity, although there are no mutations in the pore-loop complex, chimera I1G2(M), which contains the hydrophobic domain from GIRK2, exhibits normal K$^+$ selectivity. Mutation of two amino acids that are unique in the pore-loop complex of GIRK1 (F137S and A143T) restores K$^+$ selectivity and eliminates the inhibition by extracellular local anesthetics, suggesting that the pore-loop complex prevents QX-314 from reaching the intrapore site. Alanine mutations in the extracellular half of the M2 transmembrane domain alter QX-314 inhibition, indicating the M2 forms part of the intrapore binding site. Finally, the inhibition of G-protein-activated currents by intracellular QX-314 appears to be different from that observed in nonselective GIRK channels. The results suggest that inward rectifiers contain an intrapore-binding site for local anesthetic that is normally inaccessible from extracellular charged local anesthetics.

INTRODUCTION

Many inhibitory neurotransmitters exert their actions, in part, by stimulating G-protein-coupled neurotransmitter receptors and activating G-protein-gated inwardly rectifying K$^+$ (GIRK) channels (Hille, 1992; Nicoll et al., 1990; North, 1989). Near the cell's resting membrane potential, a small efflux of K$^+$ ions flows through GIRK channels and reduces membrane excitability (Hille, 1992). GIRK channels are expressed in a variety of cell types, including cardiac, brain, and endocrine tissues (Doupnik et al., 1995). In the heart, parasympathetic activation slows the heart rate by opening atrial muscarinic GIRK channels (Harris and Hutter, 1956; Trautwein and Dudel, 1958). In the brain, GIRK channels are postulated to be an important regulator of neuronal membrane excitability. Mutant mice that lack GIRK2 channels and GABA$_B$ receptor-activated GIRK currents are more susceptible to seizures (Signorini et al., 1997; Slesinger et al., 1997).

Four different mammalian GIRK channels have been identified thus far, GIRK1–GIRK4 (Kir3.1–Kir3.4) (Doupnik et al., 1995). Although GIRK2, GIRK3, and GIRK4 channel subunits form homomultimers in heterologous expression systems (Duprat et al., 1995; Kofuji et al., 1995; Krapivinsky et al., 1995a; Velimirovic et al., 1996), the GIRK1 subunit does not appear to form homomultimers (Hedin et al., 1996). In *Xenopus* oocytes, GIRK1 co-assembles with an endogenous GIRK subunit, XIR, to form func-

tional heteromultimers on the membrane surface (Hedin et al., 1996), whereas in mammalian cells, GIRK1 subunits fail to express on the membrane surface (Kennedy et al., 1996; Philipson et al., 1995). By contrast, expression of GIRK2 cRNA in *Xenopus* oocytes gives rise to large basal and G-protein-activated inwardly rectifying K$^+$ currents, indicating that GIRK2 channels form homomultimers (Kofuji et al., 1995; Lesage et al., 1995; Slesinger et al., 1996). GIRK channels are opened by the direct interaction of G protein G$_{\beta\gamma}$ subunits with the N- and C-terminal domains of GIRK (Huang et al., 1995; Inanobe et al., 1995; Krapivinsky et al., 1995b; Kunkel and Peralta, 1995). In addition to the cytoplasmic N- and C-terminal domains, GIRK channels possess two putative membrane-spanning domains (M1 and M2) (Kubo et al., 1993) and a highly conserved pore-loop complex that is involved in ion selectivity (Kofuji et al., 1996b; Slesinger et al., 1996).

In the developmentally impaired *weaver* mouse, a glycine-to-serine mutation was identified in the pore-loop complex of GIRK2 (G156S, referred to as GIRK2^{wv}) (Patil et al., 1995). The G156S mutation disrupts the ion selectivity of GIRK2 channels (Kofuji et al., 1996b; Slesinger et al., 1996) and appears to initiate the cellular changes that underlie the cell death observed in *weaver* mouse cerebellum (Kofuji et al., 1996b; Patil et al., 1995; Slesinger et al., 1997). Surprisingly, GIRK2^{wv} channels exhibit a sensitivity to inhibition by externally applied QX-314, a permanently charged derivative of the local anesthetic lidocaine (Kofuji et al., 1996b). Local anesthetics, however, are better known for their actions on voltage-gated Na$^+$ channels (Hille, 1992). The mechanism by which QX-314 inhibits GIRK2^{wv} is not well understood. A detailed electrophysiological characterization of the QX-314 inhibition of GIRK2^{wv} channels

---

may provide insights in the structure of inwardly rectifying K^+ channels. Interestingly, intracellular application of QX-314 has been reported to inhibit G-protein-gated inwardly rectifying K^+ currents in different types of neurons (Alreja and Aghajanian, 1994; Andrade, 1991; Lambert and Wilson, 1993; Nathan et al., 1990; Otis et al., 1993; Yamada et al., 1999). These findings raise the possibility that GIRK channels possess a single binding site for local anesthetics that is accessible from the cytoplasmic side of the membrane for wild-type channels and from the extracellular side of the membrane for nonselective channels.

In this paper, two different nonselective mutant GIRK channels, GIRK2^{wv} and I1G1(M), were used to study the role of the ion selectivity filter in the inhibition produced by extracellularly applied charged local anesthetics. In addition, the inhibition of wild-type GIRK channels by intracellular QX-314 was compared with that produced by extracellular QX-314 in nonselective GIRK channels. Some of these results have been reported in abstract form (Slesinger, 1999).

MATERIALS AND METHODS

Molecular biology

I1G1(M) (referred to previously as IG$_M$); Slesinger et al., 1995) and GIRK2^{wv} (Slesinger et al., 1996) cDNA constructs were made as described previously. Chimera I1G1(M) contained amino acids 1–86 and 179–428 of IRK1 and 86–179 of GIRK1. Chimera I1G2(M) was constructed using overlapping PCR and contains amino acids 1–86 and 179–428 of IRK1 and 96–189 of GIRK2. In some experiments, a hexahistidine-tagged GIRK1 was expressed with GIRK4 in oocytes; the tag had no obvious effect on channel function. Mutations in the pore-loop complex and M2 transmembrane domain were constructed using the PCR overlap technique. The numbering nomenclature for the mutants refers to the amino acid number in GIRK1. All PCR-generated products were subjected to DNA sequencing (Salk Sequencing Facility, La Jolla, CA) for potential errors generated by *Taq* polymerase. G$_{\beta1}$ and G$_{\gamma2}$ subunits were used as described previously (Reuveny et al., 1994). In vitro methyl-capped cRNA was made using a T3 or T7 RNA polymerase kit (Epicentre, Madison, WI). The concentration and quality of cRNA were estimated by separating on an ethidium-stained formaldehyde gel and comparing with the RNA molecular weight marker. *Xenopus* oocytes were isolated as described previously (Slesinger et al., 1996). Stage V/VI oocytes were injected with a 46-nl solution containing cRNA for the G protein G$_{\beta1}$ (~2–8 ng) and G$_{\gamma2}$ (~2–8 ng) subunits and/or GIRK channels (0.5–5 ng). In some experiments, 13 ng of the phosphothioated oligonucleotide XHA1 was co-injected with the cRNA to suppress the expression of XIR (Hedin et al., 1996). Oocytes were incubated in 96 mM NaCl, 2 mM KCl, 1 mM CaCl$_2$, 1 mM MgCl$_2$, and 5 mM HEPES (pH 7.6 with NaOH) for 2–7 days at 18°C.

Oocyte electrophysiology

Macroscopic currents were recorded from oocytes with a two-electrode voltage-clamp amplifier (Geneclamp 500; Axon Instruments, Foster City, CA), filtered at 0.05–2 kHz, digitized (0.1–2 kHz) with a Digidata 1200 A/D interface (Axon Instruments), and stored on a laboratory computer. Electrodes were filled with 3 M KCl and had resistances of 0.4–1 MΩ. Oocytes were perfused continuously with a solution containing 90 mM XCl (X = K$^+$, Na$^+$, or NMDG), 2 mM MgCl$_2$, and 10 mM HEPES (pH

7.5 with ~5 mM XOH or HCl for NMDG). QX-314 (RBI, Ballwin, MO), QX-222 (Tocris, Natick, MA), and lidocaine (Sigma Chemical Co., St. Louis, MO) were dissolved in dH$_2$0 at a concentration of 40–50 mM and diluted before each experiment. A small chamber (0.125 × 0.600 in) with continuous, fast perfusion (5 ml/min) was used to change the extracellular solutions and was connected to a virtual ground via a 3 M KCl agarose bridge. For examining the effect of intracellular QX-314, 32.2 nl of 40 mM QX-314 dissolved in dH$_2$0 was injected into oocytes 30–60 min before recording the currents for a second time.

Analysis

For dose-response experiments, the data were normalized by dividing the current in the presence of the drug by the current in the absence of the drug (I/I_o). The normalized data were fit with the Hill equation (Eq. 1), where K_i = the concentration at which there is 50% inhibition and h = the Hill coefficient.

$$\frac{I}{I_0} = \frac{1}{1 + \left(\frac{[X]}{K_i}\right)^h} \tag{1}$$

The mean K_i and Hill coefficients were determined by fitting each set of data points individually. The time course of QX-314 inhibition was fit with a sum of two exponentials.

For the study of mutant channels, the apparent K_i was estimated using a variation of the Hill equation (Eq. 2), where $f = I/I_o$, [QX-314] = 100 μM, and h = Hill coefficient for wild-type channels (0.855).

$$K_i = \frac{[\text{QX-314}]}{\left(\frac{1-f}{f}\right)^{1/h}} \tag{2}$$

$$K_i = K_i(0)e^{z\delta FV/RT} \tag{3}$$

The voltage dependence of QX-314 was determined by plotting the K_i as a function of voltage and fitting with the Woodhull equation (Woodhull, 1973), where $K_i(0)$ = the concentration required to produce 50% inhibition at 0 mV, $z\delta$ is the equivalent electrical distance ($z = 1$ for QX-314), and F, R, and T have their usual meaning (Eq. 3). The equation assumes a negligible rate for QX-314 exiting into the cytoplasm.

The permeability ratio (P_{Na}/P_K) was calculated (Eq. 4) from the shift in zero current potential (ΔE_{rev}) that occurred from changing the extracellular solution from all K$^+$ to all Na$^+$ (Hille, 1992).

$$\Delta E_{rev} = \frac{RT}{zF} \ln\left(\frac{P_{Na}[Na]_0}{P_K[K]_0}\right) \tag{4}$$

All values are reported as mean ± SEM. Data were analyzed for statistical significance (SigmaStat 2.0) using one-way ANOVA followed by an appropriate post hoc test. Values of $p < 0.05$ were considered significant.

RESULTS

Loss of K^+ selectivity in I1G1(M) and GIRK2^{wv}

Wild-type GIRK channels showed strong inward rectification and exhibited high selectivity for K^+ ions when expressed in *Xenopus* oocytes. Macroscopic currents were measured using two-electrode voltage clamp from oocytes injected with the cRNA for GIRK1 and GIRK4 subunits and the G protein G$_{\beta1}$ and G$_{\gamma2}$ subunits (Fig. 1 *A*). Under these
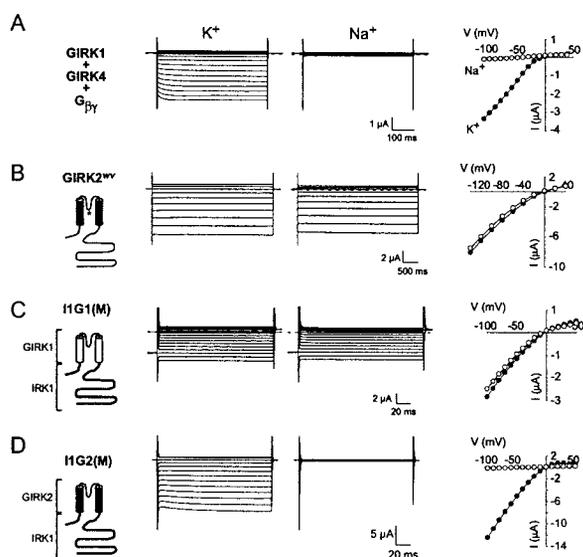
FIGURE 1 Chimera I1G1(M) loses K$^+$ selectivity. *Xenopus* oocytes were injected with the cRNA for GIRK1 and GIRK4 and the G protein G$_{\beta1}$ and G$_{\gamma2}$ subunits (*A*), for GIRK2^{wv} (*B*), for I1G1(M) (*C*), or for I1G2(M) (*D*). Macroscopic currents were recorded with a two-electrode voltage clamp from oocytes bathed in a solution containing 95 mM KCl or NaCl. Macroscopic currents were elicited by voltages steps from +50 mV to −100 mV (10-mV increments) for GIRK1+GIRK4, I1G1(M) and I1G2(M), and +40 to −140 mV (20-mV increments) for GIRK2^{wv}. The holding potential was 0 mV for *A*, *B*, and *D* and −80 mV for *C*. Dashed line indicates zero current. The current-voltage plots are shown to the right of the current traces.

conditions, large inwardly rectifying currents were observed due to G$_{\beta\gamma}$ activation of GIRK channels (Reuveny et al., 1994). To examine the K$^+$ selectivity, the macroscopic currents were elicited by voltage steps from +50 mV to −100 mV in oocytes exposed to an external solution containing all K$^+$ and then to one with all Na$^+$. GIRK heteromultimers composed of GIRK1 and GIRK4 subunits did not display any Na$^+$ current (Fig. 1 *A*). In K$^+$, note that the current-voltage plot shows little outward current at potentials positive to 0 mV, indicative of strong inward rectification (Fig. 1 *A*). As shown previously (Slesinger et al., 1996), substituting a serine for the glycine (G156S) in the pore-loop complex of GIRK2 (GIRK2^{wv}) dramatically altered the K$^+$ selectivity, allowing Na$^+$ to permeate the channel nearly equally as well as K$^+$ (Fig. 1 *B*).

Chimera I1G1(M) contains the GIRK1 hydrophobic core sequence, which includes the M1, pore-loop complex and M2, and the N- and C-terminal domains from IRK1 (Kir2.1), a G-protein-insensitive inwardly rectifying K$^+$ channel (Slesinger et al., 1995). Oocytes injected with the cRNA for I1G1(M) gave rise to large, basal inwardly rectifying K$^+$ currents (Fig. 1 *C*). Surprisingly, I1G1(M) channels sustained a large Na$^+$ current. I1G1(M) channels showed inward rectification but discriminated poorly among Na$^+$ and K$^+$ ions, like GIRK2^{wv} channels (Fig. 1, *B* and *C*). The P_K/P_{Na} permeability ratio was 0.76 ± 0.01 for

I1G1(M) (*N* = 10), as compared with 0.78 ± 0.11 for GIRK2^{wv} (Slesinger et al., 1996). By contrast, I1G2(M), which has a hydrophobic core region (M1–pore-loop-complex–M2) from GIRK2, exhibited normal K$^+$ selectivity (Fig. 1 *D*). Thus, the loss of K$^+$ selectivity in I1G1(M) appeared to be caused by amino acids in the GIRK1 channel (see below).

To examine whether nonselective channels were produced by the co-assembly of I1G1(M) with the endogenous GIRK subunit XIR, the cRNA for I1G1(M) was co-injected with an oligonucleotide antisense to XIR (KHAI). KHAI was shown by Hedin et al. (1996) to suppress the expression of the XIR. I1G1(M) channels continued to form inwardly rectifying and nonselective currents when co-expressed with KHAI (data not shown). These results suggest that I1G1(M) channels form homomultimers that lose K$^+$ selectivity.

Inhibition of I1G1(M) and GIRK2^{wv} channels by external QX-314

Kofuji et al. (1996) reported that external application of QX-314 inhibited GIRK2^{wv} channel activity when expressed in *Xenopus* oocytes. Thus, I1G1(M) channels might also exhibit sensitivity to externally applied QX-314. Several local anesthetics, QX-314, QX-222, and lidocaine (Fig. 2 *D*), were examined for their ability to inhibit I1G1(M) and
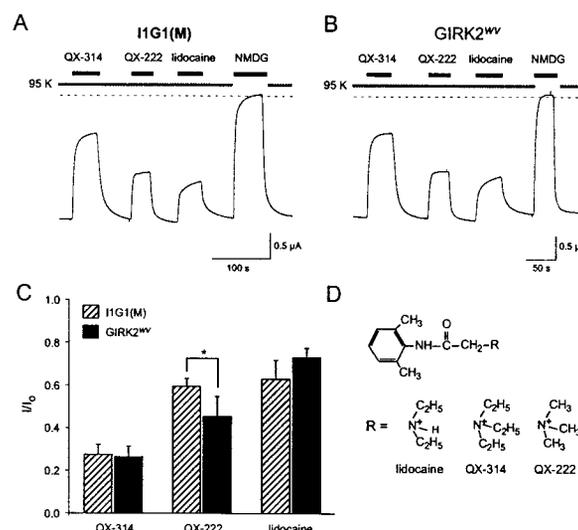
FIGURE 2 Comparison of the local anesthetic inhibition of I1G1(M) and GIRK2^{wv}. Continuous current was recorded from an oocyte injected with the cRNA for I1G1(M) (*A*) or GIRK2^{wv} (*B*). Extracellular solution contained 95 mM KCl plus 100 μM QX-314, 100 μM QX-222, or 100 μM lidocaine or 95 mM NMDG. The holding potential was −80 mV. Dashed line indicates zero current. *C*, Fractional current remaining (I/I_0) for I1G1(M) and GIRK2^{wv} channels (*N* = 4). Asterisk indicates statistical significance ($p < 0.05$) between I1G1(M) and GIRK2^{wv} using one-way ANOVA followed by Bonferroni post hoc test. *D*, Chemical structures for local anesthetics. Lidocaine is shown in the protonated form.

GIRK2^{wv} channels. The macroscopic current was recorded continuously (at −80 mV) from oocytes that were expressing I1G1(M) or GIRK2^{wv} channels (Fig. 2, *A* and *B*). Although these local anesthetics differ in the size of the terminal amine group (Fig. 2 *D*), all three local anesthetics rapidly (less than 50 s) suppressed 30–70% of the inward K^{+} current. No inward current was measured when all of the K^{+} was substituted with the large organic cation *N*-methyl-D-glucamine (NMDG) (Fig. 2, *A* and *B*). I1G1(M) and GIRK2^{wv} exhibited the same degree of inhibition as well as rank order sensitivity to inhibition by 100 μM of each local anesthetic (QX-314 > QX-222 > lidocaine; see Fig. 2 *C*). Co-expression of KHA1 oligonucleotide with the cRNA for I1G1(M) or GIRK2^{wv} had little effect on the inhibition produced by 100 μM QX-314 for I1G1(M) plus KHAI (0.42 ± 0.04; *N* = 3) and for GIRK2^{wv} plus KHAI (0.46 ± 0.22; *N* = 13). Thus, the local anesthetic binding site in I1G1(M) appears to be similar to that in GIRK2^{wv} channels.

To characterize the QX-314 binding site in more detail, the current inhibition was examined at different concentrations of QX-314 and at different voltages. Macroscopic currents were elicited by voltage steps from +50 to −140 mV in the absence and then presence of 500 μM QX-314 (Fig. 3). Voltage steps lasted 3–4 s to ensure that inhibition reached equilibrium. Heteromultimers composed of GIRK1 and GIRK4 subunits were insensitive to extracellular QX-314 (Fig. 3 *A*). By contrast, the extent of current inhibition increased with negative membrane potentials between −20 and −100 mV for I1G1(M) and GIRK2^{wv} channels (Fig. 3, *B* and *C*). At membrane potentials more negative than −100 mV, the inhibition by 500 μM QX-314 became less pro-

nounced, suggesting that there was some relief of inhibition at very negative membrane potentials. This relief of inhibition could be due to QX-314 exiting into the cytoplasm at strong hyperpolarizing membrane potentials.

To compare the sensitivity and the voltage dependence of QX-314 inhibition, the steady-state current at the end of the voltage step was divided by the current in the absence of QX-314 (I/I_0) and plotted as a function of QX-314 concentration (Fig. 4, *A* and *C*). The normalized data for each voltage were fit with the Hill equation (Eq.1, see Materials and Methods). For both channels, the K_i decreased with hyperpolarization and the Hill coefficient was at or slightly below unity (see Fig. 4 legend). The K_i was plotted as function of voltage to measure the voltage dependence (δ) of QX-314 inhibition (Fig. 4, *B* and *D*). The data points were fit with the Woodhull equation (Eq. 3), which relates the inhibition at a single site within the membrane to an equivalent electrical distance (Woodhull, 1973). The inhibition produced by QX-314 was strongly voltage dependent for both I1G1(M) and GIRK2^{wv} channels, having a δ of 0.56 and 0.76 for I1G1(M) and GIRK2^{wv} channels, respectively. The exponential fits were limited to voltages over which the relief from QX-314 inhibition (i.e., QX-314 exiting into the cytoplasm) appeared negligible. Although both channels lose K^{+} selectivity presumably through different mechanisms, the binding site for QX-314 appears to be remarkably alike.

FIGURE 3   Voltage dependence of inhibition with extracellular QX-314. *Xenopus* oocytes were injected with the cRNA for GIRK1 and GIRK4 and the G protein G$_{\beta 1}$ and G$_{\gamma 2}$ subunits (*A*), for I1G1(M) (*B*) or for GIRK2^{wv} (*C*). Macroscopic currents were recorded from oocytes bathed in 95 mM KCl in the absence and then presence of extracellular 500 μM QX-314. Macroscopic currents were elicited by voltage steps from +40 mV to −140 mV (20-mV increments). The holding potential was 0 mV. Dashed line indicates zero current. The current-voltage plots are shown to the right of the current traces.

FIGURE 4   I1G1(M) and GIRK2^{wv} channels possess similar QX-314 binding sites. The fractional current remaining (I/I_0) at different voltages is plotted as a function of QX-314 concentration for I1G1(M) (*A*; *N* = 5) and GIRK2^{wv} (*C*; *N* = 6). The smooth curves show the best fit to the Hill equation (Eq. 1). The Hill coefficient ranged from 1.00 ± 0.04 (−40 mV) to 0.73 ± 0.02 (−120 mV) for I1G1(M) and from 0.69 ± 0.14 (−40 mV) to 0.66 ± .10 (−120 mV) for GIRK2^{wv}. The K_i is plotted as a function of voltage for I1G1(M) (*B*) and GIRK2^{wv} (*D*). The smooth line shows the best fit using the Woodhull equation (Eq. 3). The $K_i(0)$ and δ were ~380 μM and 0.56 for I1G1(M) and ~420 μM and 0.76 for GIRK2^{wv}.

Inhibition of I1G1(M) and GIRK2^{wv} by extracellular Ba^{2+}

To elucidate possible differences in the pore structure between GIRK2^{wv} and I1G1(M), the sensitivity to inhibition by extracellular Ba^{2+} was examined. Current through heteromultimers composed of GIRK1 and GIRK4 subunits was nearly completely inhibited by 500 μM Ba^{2+} (Fig. 5 *A*). As shown previously, GIRK2^{wv} channels were also inhibited by 500 μM extracellular Ba^{2+} (Fig. 5 *C*) but slightly less than the inhibition of GIRK1-GIRK4 (Fig. 5 *A*) or GIRK1-GIRK2 heteromultimers (Slesinger et al., 1997). Surprisingly, I1G1(M) channels exhibited dramatically reduced inhibition with extracellular 500 μM Ba^{2+} at membrane potentials between -10 and -100 mV (Fig. 5 *B*). To quantify these differences in Ba^{2+} sensitivity, the steady-state current in the presence of Ba^{2+} was divided by the control current (I/I_o) and plotted as a function of Ba^{2+} concentration. The data points were fit with the Hill equation (Eq. 1) to determine the K_i and Hill coefficient. GIRK2^{wv} channels were less sensitive to inhibition by ex-

tracellular Ba^{2+} than heteromultimers composed of GIRK1 and GIRK4 (K$_i$ = 234 $\pm$ 42 μM for GIRK2^{wv} versus 61 $\pm$ 20 μM for GIRK1-GIRK4 heteromultimer). By contrast, I1G1(M) showed little inhibition with 3 mM Ba^{2+} and had an extrapolated K_i of $\sim$50 mM Ba^{2+}. Similar to the inhibition by QX-314, co-expression of the KHA1 oligonucleotide had little effect on the inhibition produced by Ba^{2+}. These results suggests that pore structure of GIRK2^{wv} channels is not identical to that of I1G1(M), even though both channels lose K$^+$ selectivity and have similar local anesthetic binding sites.

The remaining experiments focused on the QX-314 inhibition of I1G1(M) channels because GIRK2^{wv} channels were toxic to oocytes (Slesinger et al., 1996; Tucker et al., 1996) and appeared functionally similar to I1G1(M) channels.

Time course of inhibition by extracellular QX-314

To examine the onset of inhibition in more detail, the inward current through I1G1(M) channels was recorded in the absence and then presence of different concentrations of extracellular QX-314 (Fig. 6 *A*). The current in the presence of QX-314 was divided by the control current (Fig. 6 *B*, *inset*) and was fit best with a sum of two exponentials. The presence of two time constants suggests that more than one binding site exists for QX-314. Both time constants decreased with more negative membrane potentials (Fig. 6 *B*), consistent with the voltage-dependent inhibition measured from steady-state inhibition (Fig. 4). In addition, both time constants decreased with higher concentrations of extracellular QX-314 (Fig. 6 *B*). Thus, the inhibition of I1G1(M) by QX-314 is a bimolecular reaction that is governed by voltage and concentration.

To determine whether the permeant ion had any effect on the rate of inhibition, as has been shown for inhibition by external Ba^{2+} (Hurst et al., 1995), the rate of QX-314 inhibition was measured in 15 mM extracellular KCl. Because Na$^+$ permeates I1G1(M), an equimolar concentration of NMDG was substituted for KCl. In 15 mM KCl, the reversal potential shifted to negative voltages and the current amplitude decreased (Fig. 6 *C*). The rate of inhibition followed a double-exponential time course with time constants that were indistinguishable from those obtained in 95 mM KCl (Fig. 6 *D*). Moreover, the voltage dependence of the fast and slow time constants were similar in 15 and 95 mM KCl. These results suggest that QX-314 inhibition does not depend on V-E_K and that K$^+$ does not compete directly for QX-314 binding in the pore.

If voltage drives the permanently charged QX-314 directly into the pore, then the recovery from inhibition would be expected to be voltage dependent. A standard two-pulse protocol, commonly used to examine the voltage dependence of channel inactivation, was used to study the rate of recovery from QX-314 inhibition (Fig. 6, *E* and *F*). In this voltage protocol, the membrane potential was changed from

FIGURE 5   I1G1(M) displays reduced sensitivity to inhibition by extracellular Ba^{2+}. *Xenopus* oocytes were injected with the cRNA for GIRK1 and GIRK4 and the G protein G$_{\beta 1}$ and G$_{\gamma 2}$ subunits (*A*), for I1G1(M) (*B*), or for GIRK2^{wv} (*C*). Macroscopic currents were elicited by voltage steps from $+50$ mV to -100 mV (10-mV increments). The holding potential was 0 mV for A and -80 mV for B and C. Dashed line indicates zero current. Extracellular solution was 95 mM KCl. *D*, Fractional current remaining (I/I_0) at -80 mV plotted as a function of Ba^{2+} concentration for GIRK1 + GIRK4 ($N = 6$), I1G1(M) ($N = 6$), and GIRK2^{wv} ($N = 7$). The smooth curves show the best fit with the Hill equation (Eq. 1), with a K_i of 234 $\pm$ 42 μM and Hill coefficient of 0.59 $\pm$ 0.03 for GIRK2^{wv}, with a K_i of 61 $\pm$ 20 μM and Hill coefficient of 0.69 $\pm$ 0.12 for GIRK1 + GIRK4, and with an extrapolated K_i of 50 mM and Hill coefficient of 0.66 for I1G1(M).

FIGURE 6 Time course for onset and recovery from QX-314 inhibition of I1G1(M). *A*, Inward currents were elicited by voltage pulses from +40 to −140 mV (20-mV increments) in the absence and then presence of extracellular 100 μM extracellular QX-314 in 95 mM KCl. The holding potential was 0 mV. Dashed line indicates zero current potential. *B*, inset, Time constants for the onset of inhibition determined by fitting the QX-314 current divided by the control current (QX-314/control) with a sum of two exponentials (superimposed dashed line). The QX-314/control current with 100 μM QX-314 is shown for −80, −100, −120, and −140 mV. The two time constants are plotted as a function of extracellular QX-314 concentration for the indicated voltages. *C*, Inward currents were elicited by voltage pulses from +40 to −140 mV (20-mV increments) in the absence and then presence of extracellular 100 μM QX-314 in 15 mM KCl. The holding potential was 0 mV. *D*, Time constants for the onset of inhibition plotted for 15 and 95 mM KCl. The straight line shows the best fit to the equation $A_0\exp(zF\delta/RT)$, where δ is 0.38 (τ_1, 15 KCl), 0.43 (τ_1, 95 KCl), 0.33 (τ_2, 15 KCl), and 0.2 (τ_2, 95 KCl). *E*, Time course for recovery of QX-314 inhibition of I1G1(M). A two-pulse protocol was used to measure the recovery from QX-314 inhibition. The membrane potential was shifted to −120 mV for 3 s (first pulse) to induce ∼70% inhibition by 100 μM QX-314, returned to −40, 0, or +40 mV for varying lengths of time (Δt) to allow for recovery from QX-314 inhibition, and then shifted to −120 mV for a second time to assess the extent of recovery. The interpulse holding potential was 0 mV. Current traces are superimposed following subtraction of the current recorded in NMDG to remove capacity transients and leakage current. *F*, Amplitude of the QX-314-sensitive current during the second pulse divided by the amplitude of the first pulse (normalized current) and plotted as a function of the interpulse interval, Δt ($N = 3$).

0 mV to −80 mV for 3 s (first pulse) to induce QX-314 inhibition, was returned to 0 mV for varying lengths of time to allow for recovery, and was then changed to −80 mV for a second time to assess the extent of recovery. With increasingly longer times separating the two voltage pulses, the peak current recovered to control levels (Fig. 6, *E* and *F*). The recovery of the inhibited current was plotted as a function of the time interval (Fig. 6 *E*). With a 3–4-s interval the current recovered to nearly 100% of control. The time course of recovery followed a single-exponential time course at −40 mV, where channels remain partially inhibited, and a double-exponential time course at 0 and +40 mV (Fig. 6 *F*). The rate of recovery at +40 mV was faster than that at −40 mV suggesting that QK-314 preferentially exists extracellularly. The voltage and concentration dependence of the onset and recovery rates of inhibition suggest that QX-314 binds to sites in the permeation pathway.

Mutations in pore-loop complex of I1G1(M) partially restore K$^+$ selectivity and reduce QX-314 inhibition

Chimera I1G2(M), which contains the hydrophobic domains (M1–pore-loop-complex–M2) from GIRK2, formed functional K$^+$ selective channels in *Xenopus* oocytes (Fig. 1 *D*). The loss of K$^+$ selectivity in I1G1(M) channels might be therefore caused by amino acids that are unique to GIRK1. A comparison of the amino acid sequence in the pore-loop complex of different GIRK channel subunits (Fig. 7 *A*) revealed two amino acids, F137 and A142, that are unique to GIRK1. These two amino acids were mutated to the corresponding amino acid in GIRK2. I1G1(M) channels containing either an F137S or an A142T mutation displayed significantly smaller currents in 95 mM Na$^+$ (Fig. 7, *C* and *D*). The I_{Na}/I_K ratio was ∼0.4 and ∼0.55 for I1G1(M)-F137S and I1G1(M)-A142T, respectively, as compared with 0.8 for I1G1(M) (Fig. 7 *E*). In addition, I1G1(M)-F137S and I1G1(M)-A142T both exhibited statistically significant smaller P_{Na}/P_K permeability ratios (Fig. 7 *G*). Chimera I1G1(M) containing both mutations (F137S/A142T) showed tiny Na$^+$ currents and a P_{Na}/P_K of 0.14 ± 0.04 (Fig. 7, *E–G*), as compared with a P_{Na}/P_K of 0.05 for GIRK1 and GIRK2 (Kofuji et al., 1996b). These changes in selectivity and Na$^+$ current suggest that F137 and A142 in the pore-loop of I1G1(M) altered the K$^+$ selectivity.

If K$^+$ selectivity is nearly completely restored by mutating two amino acids in the pore-loop of I1G1(M), then the inhibition produced by extracellular local anesthetics might be impaired. To test this hypothesis, the effects of 500 μM

Smooth line shows the best fit with a single exponential for −40 mV (τ_1 = 0.97 ± 0.17 s) and a sum of two exponentials for 0 mV (τ_1 = 0.37 ± 0.03 s and τ_2 = 1.68 ± 0.57 s) and +40 mV (τ_1 = 0.26 ± 0.05 s and τ_2 = 1.18 ± 0.46 s).
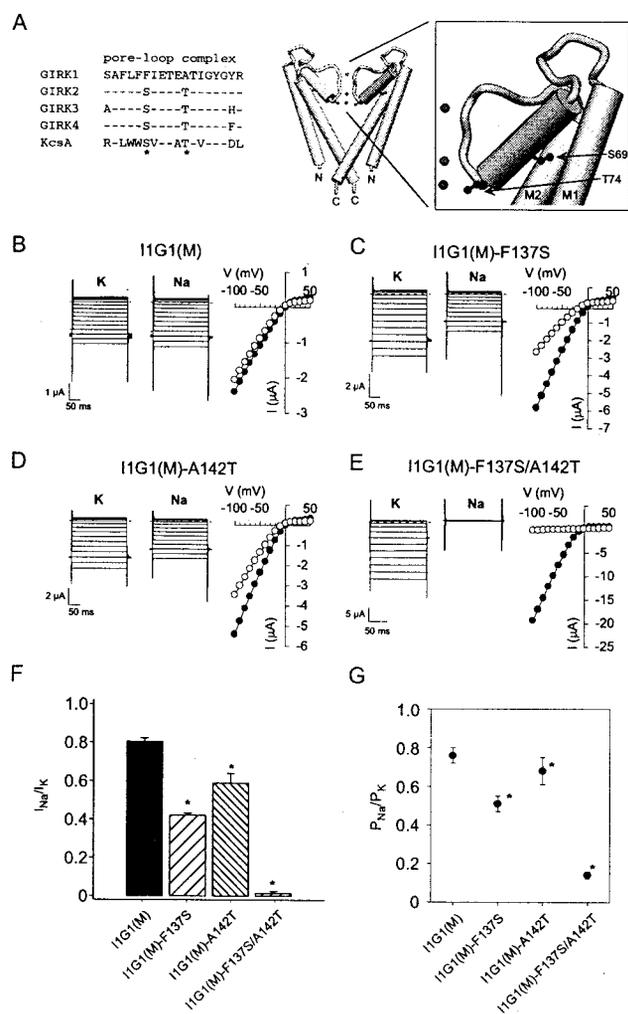
FIGURE 7 Two amino acids in the pore-loop complex of I1G1(M) are involved in determining K^+ selectivity. *A*, Alignment of the amino acids in the pore-loop complex of GIRK1, GIRK2, GIRK3, GIRK4, and KcsA channels. F137 and A142 in GIRK1 are indicated by the asterisks. Dashes indicate 100% conservation with GIRK1. The structure of KcsA is shown with two of the four subunits. The enlargement shows the position and side chain of the amino acids in KcsA that are homologous to those in GIRK1 and the three K^+ ions in the pore. Note that the side chain of S69 of KcsA, which is F137 in GIRK1, points away from the pore and interacts with M1 and M2 transmembrane domains. *B–G*, *Xenopus* oocytes were injected with the cRNA for I1G1(M) (*B*), I1G1(M)-F137S (*C*), I1G1(M)-A142T (*D*), or I1G1(M)-F137S/A142T (*E*). Macroscopic currents were elicited by voltage steps from +50 mV to −100 mV (10-mV increments) in 95 KCl or 95 NaCl. The current-voltage plot is shown to the right. *F*, Ratio of I_{Na} to I_K at −80 mV is shown. Asterisks indicate statistically significant differences ($p < 0.05$) from I1G1(M), using one-way ANOVA followed by Bonferroni post hoc test ($N = 3–8$). *G*, Plot of the P_{Na}/P_K permeability ratio determined from the change in the zero-current potential in 95 mM NaCl and 95 mM KCl (Eq. 4). All mutant I1G1(M) channels showed a statistically significant shift in the P_{Na}/P_K from that of I1G1(M) ($N = 10–11$).

QX-314, QX-222, and lidocaine on the mutant I1G1(M) channels were examined (Fig. 8). Whereas QX-314 inhibited >80% of the current through I1G1(M) channels, QX-
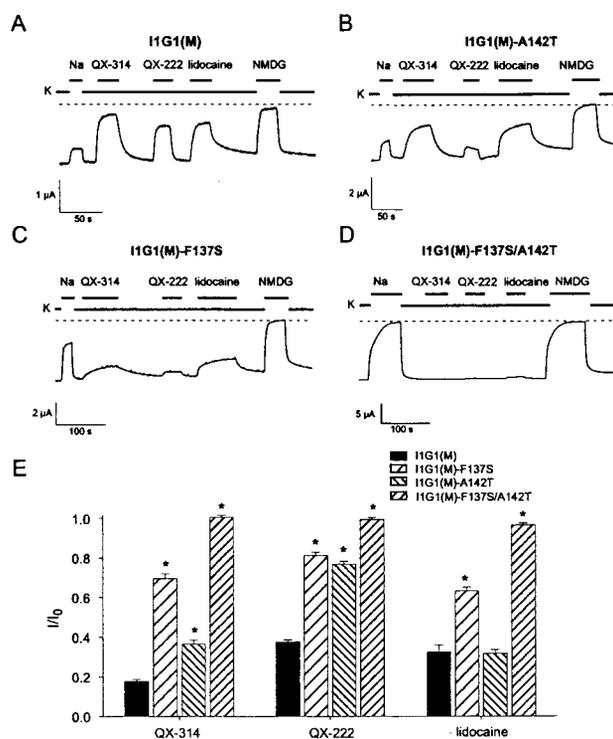
FIGURE 8 Increase in K^+ selectivity is associated with reduced sensitivity to inhibition by extracellular QX-314. Continuous currents were recorded from oocytes injected with the cRNA for I1G1(M) (*A*), I1G1(M)-F137S (*B*), I1G1(M)-A142T (*C*), or I1G1(M)-F137S/A142T (*D*). Oocytes were perfused continuously with 95 mM KCl (*solid bar*), with 95 mM NaCl, with 100 μM QX-314, QX-222 or lidocaine in 95 mM KCl, or with 95 mM NMDG. The holding potential was −80 mV. Dashed line indicates zero current. *E*, Bar graph showing the average fractional current remaining following extracellular exposure to each local anesthetic. Asterisks indicate statistically significant differences ($p < 0.05$) from I1G1(M), using one-way ANOVA followed by Bonferroni post hoc test ($N = 3–8$).

314 reduced the current by only 30% and 60% for I1G1(M)-F137S and I1G1(M)-A142T, respectively. I1G1(M)-F137S and I1G1(M)-A142T channels also showed significantly less inhibition by extracellular QX-222 than I1G1(M) (20% vs. 60%). More importantly, the K^+-selective I1G1(M)-F137S/A142T double mutant was insensitive to extracellular local anesthetics (Fig. 8, *D* and *E*), similar to wild-type channels. Thus, the inhibition produced by local anesthetics decreased as the K^+ selectivity improved, indicating that the inhibition by extracellular QX-314 is tightly linked to K^+ selectivity.

Alanine substitution in the M2 transmembrane domain of I1G1(M)

The strong voltage dependence of QX-314 inhibition indicates that QX-314 moves ~60% within the electric field, where it could potentially interact with amino acids in the M2 transmembrane domain. The M2 transmembrane domain forms part of the inner vestibule of inward rectifiers

(Lu and MacKinnon, 1994; Reuveny et al., 1996; Stanfield et al., 1994). In addition, mutagenesis studies of voltage-gated Na^+ channels have localized the local anesthetic binding site to the S6 transmembrane domain (Ragsdale et al., 1996; Sunami et al., 1997), which is homologous to M2 transmembrane domain in GIRK channels. Thus, the M2 transmembrane domain in I1G1(M) might serve as part of the local anesthetic binding site.

To examine this possibility, each amino acid in the M2 transmembrane domain of I1G1(M) was mutated individually to alanine and examined for a change in the sensitivity to the inhibition produced by extracellular QX-314. The apparent K_i was estimated using a form of the Hill equation (Eq.2, see Materials and Methods). For comparison among different batches of oocytes, the K_i for each mutant channel was normalized to the K_i for I1G1(M) channels that were expressed in the same batch of oocytes (Table 1). Five mutations in I1G1(M) (G158A, I159A, L163A, L168A, and I177A) decreased significantly (approximately twofold) the sensitivity to inhibition by QX-314. By contrast, six mutations (F162A, Q165A, I167A, G169A, I171A, and G178A) increased significantly the sensitivity to inhibition by extracellular QX-314 nearly twofold (Table 1). Interestingly, the

elimination of the negative charge at D173 had no effect on QX-314 inhibition (Table 1).

Inhibition of I1G1(M) by intracellular QX-314

Intracellular application of QX-314 inhibits neuronal G-protein-sensitive inwardly rectifying K^+ currents (Alreja and Aghajanian, 1994; Andrade, 1991; Nathan et al., 1990; Otis et al., 1993; Yamada et al., 1999). The effect of intracellular QX-314 on cloned GIRK channels has not been studied extensively. To examine the possible inhibition by intracellular QX-314, carbachol-induced currents were recorded first, QX-314 was then injected directly into oocytes, and carbachol-induced currents were recorded from the same oocyte for a second time. Based on a volume of ~ 1 μl (Sunami et al., 1997), a 32.2-nl injection of 40 mM QX-314 would produce a final concentration of ~ 1250 μM. Intracellular QX-314 reduced the early component of the carbachol-induced current (at -80 mV) by $\sim 75\%$ (Fig. 9, C and D). The same concentration of QX-314, however, inhibited only $\sim 20\%$ of the current through chimera I1G1(M) (Fig. 9, A and D), a nearly fourfold change in sensitivity. By contrast, 1250 μM of extracellular QX-314 would be expected

TABLE 1   Inhibition of I1G1(M) alanine mutants by QX-314

Mutation in M2	$K_i$mut/$K_i$wt		$\Delta\Delta G^\dagger$ (kcal/mol)
	Mean ± SEM	N	
I1G1 (M)	1.00 ± 0.11	10	0
G158A	***1.71** ± 0.16	5	**0.31**
I159A	***1.79** ± 0.13	7	**0.34**
I160A	0.82 ± 0.04	5	−0.12
L161A	1.29 ± 0.16	5	0.15
F162A	***0.47** ± 0.04	10	**−0.44**
L163A	***2.16** ± 0.16	8	**0.45**
F164A	0.95 ± 0.09	7	−0.03
Q165A	***0.36** ± 0.03	5	**−0.59**
S166A	0.85 ± 0.07	5	−0.10
I167A	***0.51** ± 0.12	5	**0.39**
L168A	***1.72** ± 0.10	5	**0.32**
G169A	***0.34** ± 0.07	6	**−0.63**
S170A	0.94 ± 0.09	5	−0.04
I171A	***0.53** ± 0.05	8	**−0.37**
V172A	0.70 ± 0.05	8	−0.21
D173A	0.82 ± 0.06	5	−0.12
A174T	0.81 ± 0.02	10	−0.13
F175A	0.95 ± 0.06	5	−0.03
L176A	1.06 ± 0.04	5	0.03
I177A	***1.45** ± 0.05	7	**0.22**
G178A	***0.54** ± 0.07	8	**−0.36**
C179A	1.28 ± 0.11	5	0.15

The amino acid number refers to the amino acid in GIRK1. The K_i for each I1G1(M) mutant was estimated using a modification of the Hill equation and divided by the K_i for I1G1(M) determined in the same batch of oocytes (Eq. 2).

* Statistically significant difference in the K_i for mutant I1G1(M) channel as compared with the K_i for I1G1(M) ($p < 0.05$, using one-way ANOVA followed by Bonferroni post hoc test).

† $\Delta\Delta G = RT\ln(K_i\text{mut}/K_i\text{wt})$.
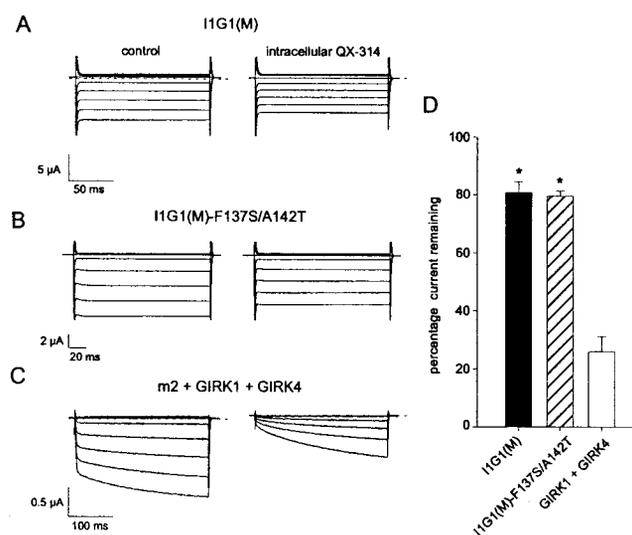
FIGURE 9   I1G1(M) loses sensitivity to inhibition by intracellular QX-314. Oocytes were injected with the cRNA for I1G1(M) (A), I1G1(M)-F137S/A142T (B), or GIRK1 plus GIRK4 along with the m2 muscarinic receptor (C). The current responses elicited by voltage steps between $+60$ and -100 mV (20-mV increments) are shown before and then 30–60 min after the injection of 32.2 nl of 40 mM QX-314. The holding potential was 0 mV. The carbachol-induced ($+$carb minus agonist-independent basal) currents are shown for GIRK1/GIRK4. Note the slow activation upon hyperpolarizing to -100 mV is more pronounced after intracellular injection of QX-314. D, Average fractional current remaining after injecting intracellular QX-314. The current was measured 10 ms after the voltage step to minimize contribution from relief of inhibition at negative membrane potentials ($N = 7$–10). Asterisks indicate statistically significant differences ($p < 0.05$) from GIRK1/4, using one-way ANOVA followed by Bonferroni post hoc test.

to inhibit >90% of the current through I1G1(M) channels (Fig. 2). The K^+-selective, double mutant I1G1(M)-F137S/A142T also showed little inhibition with intracellular QX-314 (Fig. 9, *B* and *D*). These results suggest that the local anesthetic binding site in I1G1(M) is inaccessible from the cytoplasmic side of the membrane.

DISCUSSION

There are three main findings in this paper. First, chimera I1G1(M) unexpectedly loses K^+ selectivity, although there are no mutations in the chimera sequence. Second, the loss of K^+ selectivity in I1G1(M) occurs coincidentally with an acquired sensitivity to inhibition by extracellular QX-314. Mutations that restore K^+ selectivity in I1G1(M) eliminate the inhibition by extracellular QX-314. Third, the inhibition of wild-type GIRK channels by intracellular QX-314 appears to be different from that produced by extracellular QX-314 in nonselective GIRK channels. The results are discussed in terms of a model in which the pore-loop complex must be properly positioned to maintain high K^+ selectivity and prevent large cations from reaching an intrapore binding site.

Loss of ion selectivity in chimera I1G1(M) caused by amino acids in the pore-loop complex

Both I1G1(M) and GIRK2[wv] channels lose the ability to discriminate among K^+ and Na^+ ions when expressed in *Xenopus* oocytes. In GIRK2[wv], a G156S mutation exists in the GYG sequence of the pore-loop complex (Patil et al., 1995), a region that is highly conserved among all K^+ channels and is critical for maintaining high K^+ selectivity (Heginbotham et al., 1994; Slesinger et al., 1996). The loss of K^+ selectivity in chimera I1G1(M), however, was unexpected because I1G1(M) does not contain site-specific mutations in the pore-loop complex or anywhere else in the channel. There are several plausible explanations for the loss of K^+ selectivity in I1G1(M).

First, the loss of K^+ selectivity could arise from the co-assembly of I1G1(M) with XIR, the endogenous GIRK subunit in oocytes. This explanation is unlikely because co-injecting the cRNA for I1G1(M) with an oligonucleotide that is antisense to XIR did not prevent the expression of inwardly rectifying Na-permeable and QX-314-sensitive ion channels (Hedin et al., 1996). Moreover, expression of I1G1(M) yielded large currents, unlike the small currents recorded from oocytes injected with the cRNA for GIRK1 (Hedin et al., 1996). A second possible explanation is that the N- and C-terminal domains of IRK1 are incompatible with the hydrophobic core domains of GIRK1 in I1G1(M). The loss of K^+ selectivity in I1G1(M) channels, however, was not associated with a large change in the inward recti-

fication, suggesting that these regions changed little in I1G1(M).

A more likely explanation for the loss of K^+ selectivity in I1G1(M) is that the combination of four identical pore-loop complexes from GIRK1 is incompatible with high K^+ selectivity. First, Silverman et al. (1998) reported that a GIRK4 chimeric channel containing the pore-loop complex from GIRK1 was permeable to Na^+, like I1G1(M). Second, a chimera composed of GIRK2 in the core region, I1G2(M), was shown to be K^+ selective in this paper. Third, mutations of two amino acids that are unique to GIRK1 (F137 and A142) dramatically improved the K^+ selectivity of I1G1(M) when mutated to the homologous amino acids in GIRK2. The F137S mutation in GIRK1, in particular, was implicated previously in the slow activation kinetics and heteromeric assembly of GIRK channels in *Xenopus* oocytes (Chan et al., 1996; Kofuji et al., 1996a). Chan et al. (1996) also found that GIRK1-F137S could express on the surface of oocytes as a homomultimer. At present, the mechanism by which a serine substitution in the pore-loop complex alters these properties of GIRK channels is not well understood.

Assuming that the pore structure of GIRK channels is similar to that of the bacterial K^+ channel, KcsA, the homologous amino acids (S69 and T74 in KcsA) in the pore-loop helix are positioned where they can potentially affect K^+ selectivity (Fig. 7 *A*). In KcsA, S69 is buried in the protein core between the pore-loop helix and the M1 and M2 transmembrane domains and contacts the main-chain carbonyl oxygens and side chains of L40 and S44 of M1 and partly V95 of M2. The bulkier phenylalanine could disrupt the packing of the protein, producing a large change in the backbone carbonyl oxygens in the GYG sequence, which must be positioned accurately to favor stabilizing unhydrated K^+ ions versus smaller unhydrated Na^+ ions (Doyle et al., 1998). The shift in the GYG must be large enough (~10 Å) to allow QX-314 to reach the intrapore binding site. The T74 in KcsA, on the other hand, faces the pore and may be involved in inhibition by Ba^{2+} (Doyle et al., 1998). The weak inhibition of I1G1(M) by extracellular Ba^{2+} might be due to the presence of an alanine at position 142, as compared with the more Ba^{2+}-sensitive GIRK2[wv], which has a threonine at the homologous position. That A142T must be combined with F137S to restore K^+ selectivity in I1G1(M) suggests that the bulkier threonine is structurally more compatible than alanine for maintaining K^+ selectivity.

An intrapore binding site for extracellular QX-314 in nonselective GIRK channels

The second main finding in this paper is that nonselective GIRK channels, in general, appear to be sensitive to inhibition by extracellular QX-314. The most parsimonious explanation for the acquired sensitivity is that GIRK channels possess an intrapore binding site that is normally inac-

cessible to permanently charged local anesthetics applied from the extracellular side of the membrane. If we suppose that a loss of ion selectivity occurs when the position of the critical GYG in the pore-loop complex is altered, then permanently charged local anesthetics could move past the misaligned selectivity filter to a binding site deep within the pore. Consistent with this conclusion, the mutations in the pore-loop helix that restored K^+ selectivity also dramatically reduced the inhibition produced by all three local anesthetics. The selectivity filter of Na^+ channels may serve a similar role. Sunami et al. (1997) reported that mutations in the selectivity filter of skeletal muscle Na^+ channels exposed an intrapore binding site for QX-314. Similarly, Adams et al. (1999) recently reported that a mutation in the pore-loop complex of a Na^+ channel altered Na^+ selectivity and revealed a voltage-dependent inhibition by extracellularly applied tetraethylammonium (TEA). Thus, by virtue of the strong ion selectivity in these ion channels, the selectivity filter also prevents large, charged cations from reaching the central pore cavity.

Although the mechanism underlying the change in ion selectivity in I1G1(M) and GIRK2^{wv} is likely different, both channels are inhibited by extracellularly applied local anesthetics. Most parameters of QX-314 inhibition (e.g., $K_i(0)$, Hill coefficient, voltage dependence, and rank order sensitivity to inhibition by QX-222, QX-314, or lidocaine) were indistinguishable between I1G1(M) and GIRK2^{wv}, suggesting that the local anesthetic binding sites in GIRK1 and GIRK2 are similar. Like GIRK2^{wv}, GIRK4 channels containing the *weaver* mutation also lose K^+ selectivity and become sensitive to inhibition by extracellular QX-314 (Silverman et al., 1996). The sensitivity to inhibition by extracellular QX-314 may be a general feature of nonselective GIRK channels.

The voltage dependence of QX-314 inhibition indicates that QX-314 binds to a site within the pore that senses more than half the electric potential drop across the membrane. In voltage-gated K^+ channels, the majority of the voltage drop occurs across the pore-loop complex (Yellen et al., 1991). Thus, QX-314 likely moves to a site deep within the pore, just cytoplasmic to the pore-loop complex. In fact, the upper half of the M2 transmembrane domain may comprise part of the binding site for QX-314. Of the 21 alanine substitutions studied in I1G1(M), 11 significantly shifted the sensitivity to inhibition by QX-314 by approximately ± 0.4 kcal/mol ($\Delta \Delta G$). These $\Delta \Delta G$ values are comparable to those (0.4–1.9 kcal/mol) reported for changes in QX-314 inhibition that were produced by mutations in the S6 transmembrane domain of voltage-gated Na^+ channels (Ragsdale et al., 1996; Sunami et al., 1997). In Ca^{2+} channels, alanine substitutions in the S6 transmembrane domain produced 0.4–0.94-kcal/mol changes in the sensitivity to diltiazem inhibition (Kraus et al., 1998). Different types of amino acid substitutions in the M2 of I1G1(M) might result in larger $\Delta \Delta G$ values.

When arranged into an α-helix, six of the amino acids that shifted the sensitivity of QX-314 inhibition (G158, I159, F162, Q165, G169, and I177) cluster along one face of the helix. Based on studies that have systematically mutated the M2 transmembrane domain of inwardly rectifying K^+ channels (Choe et al., 1995; Collins et al., 1997; Loussouarn et al., 2000; Lu et al., 1999), L163, Q165, G169, and I177 would be expected to face the pore and are in a good position to affect QX-314 binding. In the model proposed by Minor et al. (1999), four of the amino acids (G158, F162, Q165, and G169) would be at M1-M2 helix contact points and three would face the pore (K159, L163, and I177). The majority of the pore-facing amino acids that changed QX-314 were hydrophobic, suggesting that the dimethylphenyl moiety of QX-314 might interact preferentially with I1G1(M). Using the KcsA structure as a model for inward rectifiers, the internal pore of a GIRK channel is likely a water-filled cavity lined with hydrophobic amino acids, which is large enough (10 Å) to accommodate either TEA or QX-314 (Doyle et al., 1998). In fact, both TEA and QX-314 bind to an intrapore binding site in voltage-gated K^+ channels (Baukrowitz and Yellen, 1996). The hydrophobic environment of the intrapore cavity of GIRK channels may therefore comprise the binding site for QX-314.

Comparison with inhibition by intracellular QX-314

In neurons (Andrade, 1991; Lambert and Wilson, 1993; Yamada et al., 1999) and *Xenopus* oocytes (this study), activation of GIRK currents is inhibited by high concentrations of intracellular QX-314. I1G1(M) channels, however, showed fourfold less inhibition to intracellular QX-314 than did wild-type GIRK channels. Even the K^+-selective I1G1(M)-F137S/A142T showed little inhibition with intracellular QX-314, indicating that lack of K^+ selectivity in I1G1(M) did not account for the change in sensitivity to intracellular QX-314. I1G1(M) channels are constitutively active and no longer require G proteins (Slesinger et al., 1995). The lack of inhibition by intracellular QX-314 could be therefore related to the loss of G-protein-gating in I1G1(M). Consistent with this conclusion, a recent study with membrane-permeant local anesthetics indicated that local anesthetics inhibit GIRK channels but not other inwardly rectifying K^+ channels by interfering with the gating underlying G protein or ethanol activation of GIRK channels (Zhou and Slesinger, 2000). The mechanism underlying inhibition of nonselective GIRK channels with extracellular QX-314, therefore, appears to be different from that governing inhibition of wild-type GIRK channels with intracellular QX-314.

REFERENCES

Adams, C. M., M. P. Price, P. M. Snyder, and M. J. Welsh. 1999. Tetraethylammonium block of the BNC1 channel. *Biophys. J.* 76: 1377–1383.

Alreja, M., and G. K. Aghajanian. 1994. QX-314 blocks the potassium but not the sodium-dependent component of the opiate response in locus coeruleus neurons. *Brain Res.* 639:320–324.

Andrade, R. 1991. Blockade of neurotransmitter-activated K^+ conductance by QX-314 in the rat hippocampus. *Eur. J. Pharmacol.* 199:259–262.

Baukrowitz, T., and G. Yellen. 1996. Use-dependent blockers and exit rate of the last ion from the multi-ion pore of a K^+ channel. *Science.* 271:653–656.

Chan, K. W., J. L. Sui, M. Vivaudou, and D. E. Logothetis. 1996. Control of channel activity through a unique amino acid residue of a G protein-gated inwardly rectifying K^+ channel subunit. *Proc. Natl. Acad. Sci. USA.* 93:14193–14198.

Choe, S., C. F. Stevens, and J. M. Sullivan. 1995. Three distinct structural environments of a transmembrane domain in the inwardly rectifying potassium channel ROMK1 defined by perturbation. *Proc. Natl. Acad. Sci. USA.* 8292:12046–12049.

Collins, A., H.-H. Chuang, Y. N. Jan, and L. Y. Jan. 1997. Scanning mutagenesis of the putative transmembrane segments of $K_{ir}2.1$, an inward rectifier potassium channel. *Proc. Natl. Acad. Sci. USA.* 94: 5446–5460.

Doupnik, C. A., N. Davidson, and H. A. Lester. 1995. The inward rectifier potassium channel family. *Curr. Opin. Neurobiol.* 5:268–277.

Doyle, D. A., J. M. Cabral, R. A. Pfuetzner, A. Kuo, J. M. Gulbis, S. L. Cohen, B. T. Chait, and R. MacKinnon. 1998. The structure of the potassium channel: molecular basis of K^+ conduction and selectivity. *Science.* 280:69–77.

Duprat, F., F. Lesage, E. Guillemare, M. Fink, J.-P. Hugnot, J. Bigay, M. Lazdunski, G. Romey, and J. Barhanin. 1995. Heterologous multimeric assembly is essential for K^+ channel activity of neuronal and cardiac G-protein-activated inward rectifiers. *Biochem. Biophys. Res. Commun.* 212:657–663.

Harris, E. J., and O. F. Hutter. 1956. The action of acetylcholine on the movements of potassium ions in the sinus venosus of the frog. *J. Physiol.* 133:58P–59P.

Hedin, K. E., N. F. Lim, and D. E. Clapham. 1996. Cloning of a *Xenopus laevis* inwardly rectifying K^+ channel subunit that permits GIRK1 expression of I_{KACh} currents in oocytes. *Neuron.* 16:423–429.

Heginbotham, L., Z. Lu, T. Abramson, and R. MacKinnon. 1994. Mutations in the K^+ channel signature sequence. *Biophys. J.* 66:1061–1067.

Hille, B. 1992. Ionic Channels of Excitable Membranes. Sinauer, Sunderland, MA.

Huang, C. L., P. A. Slesinger, P. J. Casey, Y. N. Jan, and L. Y. Jan. 1995. Evidence that direct binding of $G\beta\gamma$ to the GIRK1 G protein-gated inwardly rectifying K^+ channel is important for channel activation. *Neuron.* 15:1133–1143.

Hurst, R. S., R. Latorre, L. Toro, and E. Stefani. 1995. External barium block of Shaker potassium channels: evidence for two binding sites. *J. Gen. Physiol.* 106:1069–1087.

Inanobe, A., K.-I. Morishige, N. Takahashi, H. Ito, M. Yamada, T. Takumi, H. Nishina, K. Takahashi, Y. Kanaho, T. Katada, and Y. Kurachi. 1995. $G\beta\gamma$ directly binds to the carboxyl terminus of the G protein-gated muscarinic K^+ channel, GIRK1. *Biochem. Biophys. Res. Commun.* 212:1022–1028.

Kennedy, M. E., J. Nemec, and D. E. Clapham. 1996. Localization and interaction of epitope-tagged GIRK1 and CIR inward rectifier K^+ channel subunits. *Neuropharmacology.* 35:831–839.

Kofuji, P., N. Davidson, and H. A. Lester. 1995. Evidence that neuronal G-protein-gated inwardly rectifying K^+ channels are activated by $G_{\beta\gamma}$ subunits and function as heteromultimers. *Proc. Natl. Acad. Sci. USA.* 92:6542–6546.

Kofuji, P., C. A. Doupnik, N. Davidson, and H. A. Lester. 1996a. A unique P-region residue is required for slow voltage-dependent gating of a G protein-activated inward rectifier K^+ channel expressed in *Xenopus* oocytes. *J. Physiol. Lond.* 490:633–645.

Kofuji, P., M. Hofer, K. J. Millen, J. H. Millonig, N. Davidson, H. A. Lester, and M. E. Hatten. 1996b. Functional analysis of the *weaver* mutant GIRK2 K^+ channel and rescue of *weaver* granule cells. *Neuron.* 16:941–952.

Krapivinsky, G., E. A. Gordon, K. Wickman, B. Velimirovic, L. Krapivinsky, and D. E. Clapham. 1995a. The G-protein-gated atrial K^+ channel I_{KACh} is a heteromultimer of two inwardly rectifying K^+-channel proteins. *Nature.* 374:135–141.

Krapivinsky, G., L. Krapivinsky, K. Wickman, and D. E. Clapham. 1995b. $G\beta\gamma$ binds directly to the G protein-gated K^+ channel, I_{KACh}. *J. Biol. Chem.* 270:29059–29062.

Kraus, R. L., S. Hering, M. Grabner, D. Ostler, and J. Striessnig. 1998. Molecular mechanism of diltiazem interaction with L-type Ca^{2+} channels. *J. Biol. Chem.* 273:27205–27212.

Kubo, Y., E. Reuveny, P. A. Slesinger, Y. N. Jan, and L. Y. Jan. 1993. Primary structure and functional expression of a rat G-protein-coupled muscarinic potassium channel. *Nature.* 364:802–806.

Kunkel, M. T., and E. G. Peralta. 1995. Identification of domains conferring G protein regulation on inward rectifier potassium channels. *Cell.* 83:443–449.

Lambert, N. A., and W. A. Wilson. 1993. Discrimination of post- and presynaptic GABA_B receptor-mediated responses by tetrahydroaminoacridine in area CA3 of the rat hippocampus. *J. Neurophysiol.* 69: 630–635.

Lesage, F., E. Guillemare, M. Fink, D. Fabrice, C. Heurteaux, M. Fosset, G. Romey, J. Barhanin, and M. Lazdunski. 1995. Molecular properties of neuronal G-protein-activated inwardly rectifying K^+ channels. *J. Biol. Chem.* 270:28660–28667.

Loussouarn, G., E. N. Makhina, T. Rose, and C. G. Nichols. 2000. Structure and dynamics of the pore of inwardly rectifying K(ATP) channels. *J. Biol. Chem.* 275:1137–1144.

Lu, Z., and R. MacKinnon. 1994. Electrostatic tuning of Mg^{2+} affinity in an inward-rectifier K^+ channel. *Nature.* 371:243–246.

Lu, T., B. Nguyen, X. Zhang, and J. Yang. 1999. Architecture of a K^+ channel inner pore revealed by stoichiometric covalent modification. *Neuron.* 22:571–580.

Minor, D. L., S. J. Masseling, Y. N. Jan, and L. Y. Jan. 1999. Transmembrane structure of an inwardly rectifying potassium channel. *Cell.* 96: 879–891.

Nathan, T., M. S. Jensen, and J. D. C. Lambert. 1990. The slow inhibitory postsynaptic potential in rat hippocampal CA1 neurones is blocked by intracellular injection of QX-314. *Neurosci. Lett.* 110:309–313.

Nicoll, R. A., R. C. Malenka, and J. A. Kauer. 1990. Functional comparison of neurotransmitter receptor subtypes in mammalian central nervous system. *Physiol. Rev.* 70:513–565.

North, R. A. 1989. Drug receptors and the inhibition of nerve cells. *Br. J. Pharmacol.* 98:13–28.

Otis, T. S., Y. De Koninck, and I. Mody. 1993. Characterization of synaptically elicited GABA_B responses using patch-clamp recordings in rat hippocampal slices. *J. Physiol.* 463:391–407.

Patil, N., D. R. Cox, D. Bhat, M. Faham, R. M. Myers, and A. S. Peterson. 1995. A potassium channel mutation in weaver mice implicates membrane excitability in granule cell differentiation. *Nat. Genet.* 11: 126–129.

Philipson, L. H., A. Kuznetsov, P. T. Toth, J. F. Murphy, G. Szabo, G. H. Ma, and R. J. Miller. 1995. Functional expression of an epitope-tagged G protein-coupled K^+ channel (GIRK1). *J. Biol. Chem.* 270: 14604–14610.

Ragsdale, D. S., J. C. McPhee, T. Scheuer, and W. A. Catterall. 1996. Common molecular determinants of local anesthetic, antiarrhythmic,

and anticonvulsant block of voltage-gated Na$^+$ channels. *Proc. Natl. Acad. Sci. USA.* 93:9270–9275.

Reuveny, E., Y. N. Jan, and L. Y. Jan. 1996. Contributions of a negatively charged residue in the hydrophobic domain of the IRK1 inwardly rectifying K$^+$ channel to K$^+$-selective permeation. *Biophys. J.* 70:754–761.

Reuveny, E., P. A. Slesinger, J. Inglese, J. M. Morales, J. A. Iniguez-Lluhi, R. J. Lefkowitz, H. R. Bourne, Y. N. Jan, and L. Y. Jan. 1994. Activation of the cloned muscarinic potassium channel by G protein $\beta\gamma$ subunits. *Nature.* 370:143–146.

Signorini, S., Y. J. Liao, S. A. Duncan, L. Y. Jan, and M. Stoffel. 1997. Normal cerebellar development but susceptibility to seizures in mice lacking G protein-coupled, inwardly rectifying K$^+$ channel GIRK2. *Proc. Natl. Acad. Sci. USA.* 94:923–927.

Silverman, S. K., P. Kofuji, D. A. Dougherty, N. Davidson, and H. A. Lester. 1996. A regenerative link in the ionic fluxes through the weaver potassium channel underlies the pathophysiology of the mutation. *Proc. Natl. Acad. Sci. USA.* 93:15429–15434.

Silverman, S. K., H. A. Lester, and D. A. Dougherty. 1998. Asymmetrical contributions of subunit pore regions to ion selectivity in an inward rectifier K$^+$ channel. *Biophys. J.* 75:1330–1339.

Slesinger, P. A. 1999. Internal binding site for QX314 revealed by mutations in G protein-gated inwardly rectifying K$^+$ channels. *Biophys. J.* 76:A329.

Slesinger, P. A., N. Patil, Y. J. Liao, Y. N. Jan, L. Y. Jan, and D. R. Cox. 1996. Functional effects of the mouse weaver mutation on G protein-gated inwardly rectifying K$^+$ channels. *Neuron.* 16:321–331.

Slesinger, P. A., E. Reuveny, Y. N. Jan, and L. Y. Jan. 1995. Identification of structural elements involved in G protein gating of the GIRK1 potassium channel. *Neuron.* 15:1145–1156.

Slesinger, P. A., M. Stoffel, Y. N. Jan, and L. Y. Jan. 1997. Defective γ-aminobutyric acid type B receptor-activated inwardly rectifying K$^+$

currents in cerebellar granule cells isolated from weaver and Girk2 null mutant mice. *Proc. Natl. Acad. Sci. USA.* 94:12210–12217.

Stanfield, P. R., N. W. Davies, P. A. Shelton, M. J. Sutcliffe, I. A. Khan, W. J. Brammar, and E. C. Conley. 1994. A single aspartate residue is involved in both intrinsic gating and blockage by Mg^{2+} of the inward rectifier, IRK1. *J. Physiol.* 478.1:1–6.

Sunami, A., S. C. Dudley Jr., and H. A. Fozzard. 1997. Sodium channel selectivity filter regulates antiarrhythmic drug binding. *Proc. Natl. Acad. Sci. USA.* 94:14126–14131.

Trautwein, W., and J. Dudel. 1958. Zum mechanismus der membran-wirkung des acetylcholin an der herzmuskelfaser. *Pflügers Arch.* 266:324–334.

Tucker, S. J., M. Pessia, A. J. Moorhouse, F. Gribble, F. M. Ashcroft, J. Maylie, and J. P. Adelman. 1996. Heteromeric channel formation and Ca^{2+}-free media reduce the toxic effect of the weaver Kir 3.2 allele. *FEBS Lett.* 390:253–257.

Velimirovic, B. M., E. A. Gordon, N. F. Lim, B. Navarro, and D. E. Clapham. 1996. The K$^+$ channel inward rectifier subunits form a channel similar to neuronal G protein-gated K$^+$ channel. *FEBS Lett.* 379:31–37.

Woodhull, A. M. 1973. Ionic blockage of sodium channels in nerve. *J. Gen. Physiol.* 61:687–708.

Yamada, K., B. Yu, and J. P. Gallagher. 1999. Different subtypes of GABA$_B$ receptors are present at pre- and postsynaptic sites within the rat dorsolateral septal nucleus. *J. Physiol.* 81:2875–2883.

Yellen, G., M. E. Jurman, T. Abramson, and R. MacKinnon. 1991. Mutations affecting internal TEA blockade identify the probable pore-forming region of a K$^+$ channel. *Science.* 251:939–942.

Zhou, W., and P. A. Slesinger. 2000. Bupivacaine rapidly inhibits G protein-gated inwardly rectifying K$^+$ channels. *Biophys. J.* 78:2033.A.